

Assessment of Surface Rendering with 1 DoF Vibration

Oliver Snyder^a, Rebeka Almasi^b, Cathy Fang^c, Roberta L. Klatzky^b, and George Stetten^{a*}

^aDepartment of Bioengineering, University of Pittsburgh, Pittsburgh, PA; ^bDepartment, of Psychology, Carnegie Mellon University, Pittsburgh, PA; ^cDepartment, of Mechanical Engineering, Carnegie Mellon University, Pittsburgh, PA

**george@stetten.com, 302 Benedum Hall, University of Pittsburgh, Pittsburgh PA, 412-624-7762*

Provide short biographical notes on all contributors here if the journal requires them.

Word Count: 3683

Assessment of Surface Rendering with 1 DoF Vibration

This paper describes the creation and testing of a prototype device for rendering texture, using a touch-sensitive surface consisting of a linear soft potentiometer (LSP) attached to a 3D printed platform and mounted on the cone of a 5-inch loudspeaker. Displacement of the cone is determined by finger position along the LSP. The roughness quality of rendered textures was evaluated psychophysically: A magnitude-estimation task measured how changes in the amplitude and spatial frequency of the rendered texture translated into perceptual change. A just-noticeable difference (JND) task measured the threshold for detection of change in amplitude or frequency, proportional to a base value. Magnitude estimation demonstrated sensitivity to both variables across the physical scales presented, but with stronger effects for amplitude: A doubling of frequency led to an approximate doubling of reported magnitude, whereas a 60% increase in amplitude led to an 86% increase in magnitude. The amplitude thresholds averaged 24%, whereas the frequency thresholds were substantially higher, averaging 64% but with substantial inter-participant variability. We conclude that the device has promise for conveying a broad range of vibratory effects and hence may simulate textural variations, but additional research is necessary to further its capabilities for differentiating vibrations close in frequency.

Keywords: haptic rendering, virtual reality, psychophysics, texture

Introduction

The field of haptic technology has seen a burgeoning of tools for creating virtual objects and surfaces in recent decades. Barriers remain, however, in providing devices that could augment image-based medical interventions with the sense of touch. We suggest that vibrations resulting from vertically displacing a surface with a loudspeaker in response to translation of the finger across that surface could be the basis for a low-cost, portable approach to haptic rendering, one that might ultimately be realized in a device suitable to simulate feedback from interactions otherwise represented by vision alone. The present research introduces a prototype haptic device intended for such use and

characterizes perceptual responses to the stimulation it provides.

We envision clinical applications that would use the device to measure tactile acuity and motor control, for example, to monitor diabetic neuropathy, or tremor and bradykinesia in Parkinson's disease. These tests could take place in the doctor's office, or, with the inexpensive nature of the device, in the patient's home, providing a more complete record throughout the day and thereby clues to contributing factors during activities of daily living.

Our prototype capitalizes on previous efforts to simulate surface features that can be perceived by touch [1, 2]. The resulting perceptual properties are commonly given labels such as roughness, slipperiness, and hardness [3, 4, 5]. In general, haptic devices attempt to convey a virtual surface by variations in sustained force and vibration. (Thermal cues may also be manipulated but are not considered here.) Such simulations are effective to the extent that the *sensory* signal provided by the interface evokes a *perceptual* representation of the effects of interaction with a physical world [6, 7]. As will be described below, embedded sensory receptors in human skin are highly responsive to vibration, suggesting that vibratory stimulation could be an effective medium for simulating surface properties, particularly fine structural variations that are relevant to medicine, such as with cutaneous lesions. Vibratory signals should, in principle, produce a perceptual representation of a textured surface when temporal variation in force amplitude against the finger can be perceptually conflated with spatial variation in underlying surface height, representative of texture elements [8].

The effectiveness of this approach relies on the demonstrated sensitivity of human skin to vibrotactile stimulation. Extensive studies were conducted decades ago to measure the absolute threshold for vibration, in terms of the minimal detectable amplitude, across a wide range of frequencies (see [9], e.g., for review). This body of

work identified two populations of vibration-sensitive mechanoreceptive neural fibers, terminating in distinct specialized endings that house the sensory receptors. The Meissner Corpuscles (terminals of fast acting (FA) I fibers) lie near the skin surface and are associated with low-frequency vibration detection, whereas the deeper Pacinian Corpuscles (PCs, terminals of FA II fibers) exhibit maximal sensitivity at approximately 250 Hz. More recently [10], the threshold amplitude for frequency discrimination (just-noticeable difference, or JND) at the fingertips has been measured and found to vary from 32% to 14% over the frequency range 20 Hz - 200 Hz. (The corresponding values for the hairy skin on the forearm are 36% to 17%.)

A number of findings indicate that the vibration-sensitive PCs are critical to discrimination of finely textured surfaces. In [10], differences in frequency discrimination between hairy and glabrous skin sites could be explained by relative contributions from afferents in the hair follicles and the deeper PCs. The firing of neural fibers from the PCs has been found to be phase-locked with the frequency of the stimulus, and there are strong correlations between the power spectra of skin vibrations and the responses of individual PC fibers when fine materials are stroked [11].

In order to capitalize on human vibrotactile sensitivity for haptic rendering, the essential approach is to allow a user to move an effector in space while imposing variations in force as a function of its location, according to an underlying model of a virtual surface. At suitable spatial/temporal scale, the force variation becomes a vibration tuned to human tactile sensitivity. Force-feedback devices accomplish this coupling by having the user hold a tool or insert the finger in a receptacle, in which case kinesthetic sensing contributes along with vibrations that activate rapidly adapting mechanoreceptors. Another approach is to use electrostatic or piezoelectric effects to adjust the friction on a surface explored by the bare finger [12, 13, 14, 15]. Rapidly

adapting skin mechanoreceptors have been implicated as mediators for these friction-induced effects [16].

Importantly for the present research, a 1 degree-of-freedom (DoF) model for force activation is sufficient to create a compelling illusory representation of physical texture. In a force-feedback environment, the spatial variation is programmed into a model of a physical surface with location-specific height variations. Unger and associates [17] implemented a constraint surface model, which mapped the effector contact point to the virtual surface and generated a counter-force proportional to the depth of penetration. Bodas et al [18] used the TPad [12], a piezoelectric surface-haptics device, which activates the entire surface to a friction level according to the momentary fingertip location. In common across these two quite different approaches to texture rendering, simulated gratings were found to effectively produce perceptual representations of roughness that varied systematically with geometric parameters of the simulated surface. Additional cues such as torque may enhance rendered textural effects [19] but are not necessary additions to a single axis of force variation with spatial dependence.

Strohmeier and associates [20] created a vibratory texture simulator with three elements: a 1 DoF vibrotactile actuator called the Haptuator (Tactile Labs) driven by electronic inputs from a sound card, a sliding element driven by the finger, and a linear position tracker. Pulses were adjusted in real-time to compensate for user speed, allowing control of frequency as well as amplitude, and the acoustic signal was bandpass filtered to produce variations in timbre (the audio-frequency content of individual pulses). Variations in these parameters created different impressions of intensity and textural experience.

A reason for interest in 1 DoF simulation is that it is commercially attractive, reducing the complexity, bandwidth requirements, and expense of rendering for everyday use. Landin et al. [21] described the process by which 3-dimensional data, such as those acquired from an accelerometer, are reduced to a single axis as three-to-one (321) reduction. Park and Kuchenbecker [22] described several methods by which 321 reduction might be accomplished and conducted evaluation experiments showing that the similarity structure of a set of textures was preserved across some techniques.

The present 1 DoF device, a speaker, is a promising addition to this approach. Speakers are manufactured to produce high-quality sound, for which small, linear, and accurate displacements accompanied by strong forces are essential. Although speakers have been used commonly for tactors, speakers have not, to our knowledge, been used in creating a texture renderer, which is different from a tactor in that it produces displacement in response to an input such as translational motion across its surface.

Materials and Methods

The goal of the present project was to capitalize on the demonstrated effectiveness of 1-DoF actuations to render virtual textures by inducing the sensation of texture in an inexpensive and simple device. We made use of an acoustic loudspeaker (Faital PRO 5FE120, 160 Watt) previously employed for haptic rendering of forces in surgical simulators [23, 24]. Additional capability for active exploration by the user was implemented by mounting a rigid platform containing a position sensor onto the speaker cone (Fig. 1). In response to movement across the position sensor, the speaker is moved up and down according to a preset mapping function relating finger position to speaker cone height. Thus, a virtual representation of a surface texture is presented to the user's finger. The position sensor is a linear soft potentiometer (LSP, made by SpectraSymbol)

measuring 103 x 7 mm, fully supported by a scaffolding 3D printed from rigid stereolithography (SLA) resin and glued to the cone of the speaker. The LSP senses the pressure and linear position of the user's finger on the platform, and an optical distance sensor (Vishay TCRT500L) mounted within the speaker frame measures the height of the speaker cone. Voltage signals from the LSP and optical sensor are read by a Raspberry Pi (RPi) computer through a 12-bit analog-to-digital converter (ADS1015). Output signals from the RPi pass through a 12-bit digital-to-analog converter (MCP4822) to a custom-built analog linear amplifier, which drives the speaker. The texture generation program (described below) was implemented in C, while experimental procedures and user interfaces were created in Python with the PsychoPy toolkit.

Force calibration for the speaker was performed using a digital force gauge (DS2-50N, Imada). The voltage-to-force conversion was modeled as linear with a slope of -0.393 N/V ($R^2 = 0.9969$) over a maximum displacement of 0.36 mm from the resting displacement of the speaker (see Fig. 2).

The control algorithm (see Fig. 3) was implemented to provide a maximum update rate of approximately 15 kHz, which corresponds to a maximum temporal frequency of 7.5 kHz. In each time frame, the 1-DoF finger position sensed by the LSP was mapped to a targeted platform height for the simulated surface through a pre-generated lookup table. The target height was then corrected for the actual height of the speaker cone, as sensed by the optical sensor, which allowed the device to react to changes in height due to pressure applied by the user. This process occurred iteratively throughout the user's movement across the LSP. Spatial frequencies could be stably rendered with a resolution of up to 0.9 samples per mm, with instability occurring only at higher amplitudes than used in the experiments.

Results

The capabilities of the device for eliciting a perceptual response were tested with two tasks: magnitude estimation and just-noticeable difference (JND). The magnitude-estimation task was used to measure how changes in the physical values of amplitude and frequency translated into perceptual change. As noted below, although we use the term roughness, the percept might be captured by other terms such as “buzzy.” By sweeping across a range of physical values, it is possible to derive a function relating perceived magnitude to the physical variable and extract a parametric description. The JND measured the threshold for detection of change in amplitude or frequency, as a proportion of the base value, to characterize perceptual differentiation near its limit of sensitivity.

Magnitude Estimation Task

Participants

The participants were eight young adult students from Carnegie Mellon University who participated with written informed consent according to a University-approved protocol and received credit for a Psychology requirement. They wore sound-cancelling earphones during this task. Four of the participants performed the JND task as well; there was no evidence of a difference between those performing two tasks versus one.

Procedure and design

The task was free magnitude estimation. Participants were asked on each trial to explore a texture without time limitation and indicate how rough it was. They were told that the texture was actually a vibration, and that roughness corresponded to a

combination of strong and buzzy. They could use a whole number excluding zero, fraction, or decimal, subject to the constraints that larger numbers should correspond to rougher textures and no negative number should be used.

The design created 25 vibratory textures by crossing 5 levels of peak-to-peak amplitude (.17 -.27 mm in equal intervals) with 5 levels of spatial frequency (.19 - .39 cycles/mm in equal intervals). These values were chosen to sample broadly across a stable range of the device. The stimuli were presented in a random order, without repeat, in each of two successive blocks, totaling 50 judgments per participant. There was no break in the sequence.

Experimental Results

To adjust for variations in the magnitude scale, each participant's scores were normalized by dividing by his or her mean across the entire set of trials. Figure 4 shows the normalized magnitude ratings by amplitude and frequency. An ANOVA on these factors showed both main effects were significant: frequency, $F(4, 28) = 13.77$, $p < .001$, and amplitude, $F(4, 28) = 41.23$, $p < .001$, with a non-significant interaction. The individual functions of magnitude against stimulus value (amplitude at each frequency; frequency at each amplitude) were well accounted for by linear trend analysis. Specifically, linear regression on these functions showed $r^2 > .90$ in all but two cases: magnitude vs. amplitude at the lowest frequency ($r^2 = .58$) and magnitude vs. frequency at the second-to-lowest amplitude ($r^2 = .77$).

JND Task

Participants

The participants were eight young adult students from Carnegie Mellon University who participated with written informed consent under a University-approved protocol and received credit for a Psychology requirement. They wore sound-cancelling earphones. Four of the participants performed the magnitude-estimation task as well; no systematic differences were found between those who performed two tasks versus one.

Procedure and design

The JNDs were measured with an adaptive staircase procedure using unforced choice in a decreasing sequence, targeting a 75% threshold [25]. On each trial, the participant was provided two stimuli to freely explore and indicate which was rougher. For amplitude, roughness was further described as stronger; more intense. For frequency, it was described as buzzier, faster. Exploration was undirected and unlimited in duration. If the participant was correct, the difference was reduced by a quantity D . If the participant was incorrect, it was increased by quantity $3 \cdot D$. For don't-know responses, the amplitude was increased by D . The value of D was halved after the second reversal and again after the fourth. The threshold was measured after the 8th reversal as the average value from the 4th to the 8th, minus baseline. To preclude the possibility that subtracting D could cause the comparison stimulus to jump below the baseline, we fixed a minimum difference, such that if participants reached this level the same comparison was repeated. (In principle, this sets a lower bound on the JND, but reaching the minimum occurred only four times over the entire data set, and in each case the participant reached the bound only once along a run and then failed when the same test was repeated, necessitating an increase in the tested difference.)

JNDs were measured at two baseline values of each parameter, amplitude and frequency, with the other parameter fixed. It can be seen from Figure 3 that the device

is capable of providing differential perceptual experience across a range of values for each parameter, creating a large space of possible JND measures. Taking JND measures for two baseline values of each parameter gives an indication of whether the JND values are a constant percentage of baseline, as predicted by Weber's Law. Informal pre-testing was used to select the baseline levels of each parameter, the starting values for the descending sequence of tests, and the step size of change in the algorithm, D . Amplitude JNDs were tested at a relatively low fixed frequency of .19 cycle/mm, to promote stability of the device at the high amplitudes where the descending sequence began. The two baseline amplitudes tested had peak-to-peak values of .17 mm and .25 mm. The initial amplitude level for both baselines was set to .33 mm, and the value of D was set to .017 mm. Frequency JNDs were measured with amplitude fixed at a peak-to-peak value of .25 mm; it can be seen in Figure 2 that the magnitude function is well differentiated for that level of amplitude. The baseline frequency values were .29 and .49 cycles/mm. The starting point was .29 cycles/mm above the baseline in each case, and initial D was set at .08 cycles/mm.

Experimental Results

Table 1 presents summary statistics for the JND, expressed as the just-detectable difference from the adaptive staircase as a percentage of baseline. The amplitude thresholds averaged 24%, whereas the frequency thresholds were substantially higher, averaging 64%. Note, however, that the median JND for the low frequency is considerably less than the mean. This reflects a split between three participants with very high JNDs (two over 100%), and the remaining five (JND range 16%-33%).

Figure 5 shows sample traces from two participants in the JND task. Considering the JND as a measure of discrimination success, the upper graph shows a relatively successful effort at low amplitude, yielding a JND of 20%. The lower graph

shows a participant who was less successful at high amplitude with a final threshold of 60%.

Correlations were used to assess whether participants exhibited a consistent relative JND level across the various parameters. No such tendency was found; to the contrary, the strongest correlation was a negative relation between difference thresholds at the low and high frequency level ($r = -.44, p > .05$).

Paired t-tests comparing JNDs for the low and high baseline level of each variable (amplitude, frequency) showed null effects ($ps > .25$), as is consistent with Weber's Law (i.e., by statistical criteria, the JND is a constant percentage of the base value). In contrast, when JNDs were compared across the two parameters, the JND for the high-frequency condition was significantly greater than both the high and low amplitude conditions, $t(7) = 5.55$ and $3.70, p < .001$ and $p = .007$, respectively.

Discussion

We envision an application domain in which a physician can experience feedback from a remote examination through the sense of touch. This is accomplished by a simple and inexpensive haptic device that is actuated in correspondence with the position of the user's finger, stylus, or mouse on an image of the surface being presented. The present research is intended to further the development of such haptic tools by exploring the capabilities of a 1-DoF texture renderer with very low complexity and cost. Our experiments point to both promise and problems with the textures rendered by the device.

Magnitude estimations provided evidence of sensitivity to both vibratory variables across the physical scales presented, but with stronger effects for amplitude: A doubling of frequency (from lowest to highest value) led to an approximate doubling of reported magnitude, whereas a 60% increase in amplitude led to an 86% increase in

magnitude. The greater sensitivity was still more evident in the comparative JND levels, as seen in Table 1. It should be noted, however, that there was substantial variation across individuals in frequency discrimination performance, particularly at the lower frequency level.

The amplitude JND is higher than has been reported for force (5-10% for finger pinching in [26] and elbow flexing in [27]) but comparable to JNDs reported for stiffness [28, 29]. Comparison of the frequency JNDs to the literature is somewhat more difficult, given that the rate of exploration was uncontrolled. Although exploration is known to vary with the perceiver's goal and the surface itself [30], an estimate of the rate can be made from extant values. Callier et al. [31] reported that when textures were explored for purposes of judging roughness, movement rates were centered on approximately 90 mm/sec. Assuming that rate holds here, converting the current spatial textures of .29 and .49 cycles/mm produces temporal vibrations rates on the order of 30-50 Hz. Vibratory JNDs for the fingertip reported by [7] for vibrations of 20 and 50 Hz were 32% and 19%, respectively. The current JNDs for frequency are 2-3 times that level. It would be useful to measure the scanning rate in further studies, but improved estimates are unlikely to alter the conclusion that the frequency discrimination possible with the current device falls far short of discrimination with the fingertip.

Clearly, the prototype 1-DOF device is not successful in promoting discrimination of vibratory frequency when users are queried directly, as indicated by the high JNDs. However, the magnitude judgments confirm that frequency variations across a substantial range are translated into subjectively variable roughness. While the present psychophysical testing did not include an evaluation of textural aesthetics, we have demonstrated the device and tested it informally over a wide parametric range. At

extremes of frequency and amplitude, the effect may seem more like buzz than surface, but intermediate settings can produce subjective effects of material like corduroy.

The present device has the advantage of low cost and simplicity. The resolution of the optical position sensor and the speaker-based actuator make it capable of the small changes in depth required to render texture. The fact that the speaker is capable of much greater displacement does not detract from this.

Further iterations could replace the 1-DoF tracker for finger position with a two-dimensional track-pad. It may also be possible to eliminate tracking entirely, and to control the vibrations through a temporal profile independent of user position (assuming the finger is in motion). This approach has the potential consequence that the perceived locations of surface elements will vary according to exploratory parameters such as velocity and phase. This might be problematic for textures at relatively large scale, where surface elements emerge as shapes. Because fine textures are coded as temporal signals, however, the precise location of vibratory variations should have little impact on perception at the smaller scale.

Acknowledgements

This research was supported by the National Science Foundation under Grant No. IIS-1518630

References

- [1] R. L., Klatzky, D. Pawluk, and A. Peer, "Haptic perception of material properties and implications for application," *Proceedings of the IEEE*, vol. 101, pp. 2081-2092, 2013.
- [2] W. Bergmann Tiest, "Tactual perception of material properties," *Vision Research*, vol. 50, pp. 2775–2782, 2010.

- [3] M. Hollins, R. Faldowski, S. Rao, and F. Young, "Perceptual dimensions of tactile surface texture: A multidimensional scaling analysis," *Perception and Psychophysics*, vol. 54, pp. 697-705, 1993.
- [4] M. Hollins, S. Bensmaïa, K. Karlof, and F. Young, "Individual differences in perceptual space for tactile textures: Evidence from multidimensional scaling," *Perception and Psychophysics*, vol 62, pp. 1534-1544, 2000.
- [5] W. M. Bergmann Tiest and A. M. Kappers, "Analysis of haptic perception of materials by multidimensional scaling and physical measurements of roughness and compressibility," *Acta Psychologica*, vol. 121, pp. 1-20, 2006.
- [6] J. Loomis, "Distal attribution and presence," *Presence: Teleoperators and Virtual Environments*, vol. 1, pp. 113-119, 1992.
- [7] S. Bensmaïa, M Hollins, and J. Yau, "Vibrotactile intensity and frequency information in the pacinian system: a psychophysical model," *Perception & psychophysics*, vol. 67, pp. 828–841, 2005.
- [8] H. Culbertson, J. Unwin and K. Kuchenbecker, "Modeling and rendering realistic textures from unconstrained tool-surface interactions," *IEEE Transactions on Haptics*, vol. 7, pp. 381-393, 2014.
- [9] J.D. Greenspan and S.J. Bolanowski, "The psychophysics of tactile perception and its peripheral physiological basis," In *Pain and Touch: A Volume in Handbook of Perception and Cognition*, L. Kruger (Ed.), pp. 25-103. New York: Elsevier, 1996.
- [10] D. A. Mahns, N. M. Perkins, V. Sahai, L. Robinson, and M. J. Rowe, "Vibrotactile frequency discrimination in human hairy skin," *Journal of Neurophysiology*, vol. 95, pp. 1442-50, 2006.
- [11] A. I. Weber, H. P. Saal, J. D. Lieber, J.-W. Cheng, L. R. Manfredi, J. F. Dammann III, and S. J. Bensmaia, "Spatial and temporal codes mediate the tactile perception of natural textures," *Proceedings of the National Academy of Sciences*, vol. 110, pp. 17107-17112, 2013.

- [12] L. Winfield, J. Glassmire, J. E. Colgate, and M. Peshkin, "T-PaD: Tactile pattern display through variable friction reduction," *Proceedings of World Haptics Conference 2007*, pp. 421-426, 2007.
- [13] O. Bau, I. Poupyrev, A. Israr, and C. Harrison, "TeslaTouch: Electro-vibration for touch surfaces," *Proceedings of UIST 2010*, pp. 283-292, 2010.
- [14] D. J. Meyer, M. A. Peshkin, and J. E. Colgate, "Fingertip friction modulation due to electrostatic attraction," *Proceedings of IEEE World Haptics Conference 2013*, pp. 43-48, 2013.
- [15] D. J. Meyer, M. Wiertelowski, M. Peshkin, and J. E. Colgate, "Dynamics of ultrasonic and electrostatic friction modulation for rendering texture on haptic surfaces," *Proceedings of IEEE Haptics Symposium*, pp. 63-67, 2014.
- [16] Y. Vardar, B. Güçlü, and C. Basdogan, "Effect of waveform on tactile perception by electrovibration displayed on touch screens," *IEEE Transactions on Haptics*, vol. 10, pp. 488-499, 2017.
- [17] B. Unger, R. L. Klatzky, and R. Hollis, "The physical basis of perceived roughness in virtual sinusoidal textures," *IEEE Transactions on Haptics*, vol. 6, pp. 496-505, 2013.
- [18] P. Bodas, R. F. Friesen, A. Nayak, H. Z. Tan, and R. L. Klatzky, "Roughness rendering by sinusoidal friction modulation: Perceived intensity and gradient discrimination," *Proceedings of IEEE World Haptics Conference*, pp. 443-448, 2019.
- [19] S. Aghajani Pedram, R. Klatzky, R., and P. Berkelman, "Torque contribution to haptic rendering of virtual textures," *IEEE Transactions on Haptics*, vol. 10, pp. 567-579, 2017.
- [20] P. Strohmeier and K. Hornbæk, "Generating Haptic Textures with a Vibrotactile Actuator," In *Proceedings of the 2017 CHI Conference on Human Factors in Computing Systems*, pp. 4994-5005, 2017.

- [21] N. Landin, J. M. Romano, W. McMahan, and K. J. Kuchenbecker, "Dimensional reduction of high-frequency accelerations for haptic rendering," in *Haptics: Generating and Perceiving Tangible Sensations (EuroHaptics)*, pp. 79–86. New York: Springer, 2010.
- [22] G. Park and K. J. Kuchenbecker, "Objective and subjective assessment of algorithms for reducing three-axis vibrations to one-axis vibrations," *Proceedings of IEEE World Haptics Conference*, pp. 467-472, 2019.
- [23] A. Khera, R. Lee, A. Marcovici, Z. Yu, R. L. Klatzky, M. Siegel, S. G. Shroff, G. Stetten, "One-dimensional haptic rendering using audio speaker with displacement determined by inductance," *Machines*, vol. 4, no. 9, 2016.
- [24] R. Lee, A. Marcovici, A. Khera, Z. Yu, R. L. Klatzky, M. Siegel, S. G. Shroff, and G. Stetten, "One-dimensional haptic rendering device based on an audio loudspeaker," Work in progress and demonstration, *IEEE Haptics Symposium*, April 2016.
- [25] C. Kaernbach, "Adaptive threshold estimation with unforced-choice tasks," *Attention, Perception and Psychophysics*, vol. 63, pp. 1377-1388, 2001.
- [26] X. D. Pang, H. Z. Tan, and N. I. Durlach, "Manual discrimination of force using active finger motion," *Attention, Perception and Psychophysics*, vol. 49, pp. 531-540, 1991.
- [27] L. A. Jones, "Matching forces: constant errors and differential thresholds," *Perception*, vol. 18, pp. 681-687, 1989.
- [28] L. A. Jones and I. W. Hunter, "A perceptual analysis of stiffness," *Experimental Brain Research*, vol. 79, pp. 150–156, 1990.
- [29] H. Z Tan, N. I. Durlach, G. L. Beauregard, and M. A Srinivasan, "Manual discrimination of compliance using active pinch grasp: the roles of force and work cues," *Perception and Psychophysics*, vol., 57, pp. 495–510, 1995.

- [30] Y. Tanaka, W. M. Bergmann Tiest, A. M. L. Kappers AML, and A. Sano A
“Contact force and scanning velocity during active roughness perception. *PLoS ONE* 9(3): e93363. doi:10.1371/journal.pone.0093363, 2014.
- [31] T. Callier T, H. P. Saal, E. C. Davis-Berg, S. J. Bensmaia, “Kinematics of unconstrained tactile texture exploration,” *Journal of Neurophysiology*, vol. 113, pp. 3013-3020, 2015.

Table 1. Statistical measures of JND (%) across participants for two baseline amplitudes and frequencies. (Min, Max, and SD stand for minimum, maximum, and standard deviation.)

Baseline	Min	Max	Mean	Median	SD
Amplitude: .17 mm	11	66	28.4	26.0	17.1
Amplitude: .25 mm	10	34	20.6	18.5	7.9
Freq: .29 cycle/mm	13	163	58.5	30.0	54.7
Freq: .49 cycle/mm	43	97	69.9	69.5	20.9

Figure 1

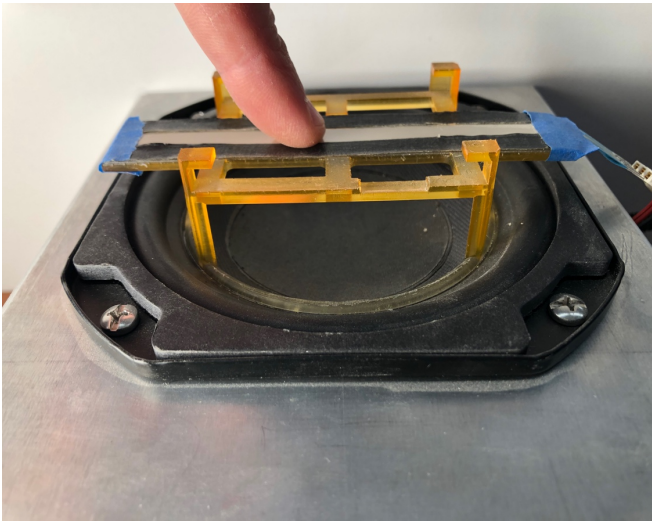


Figure 2

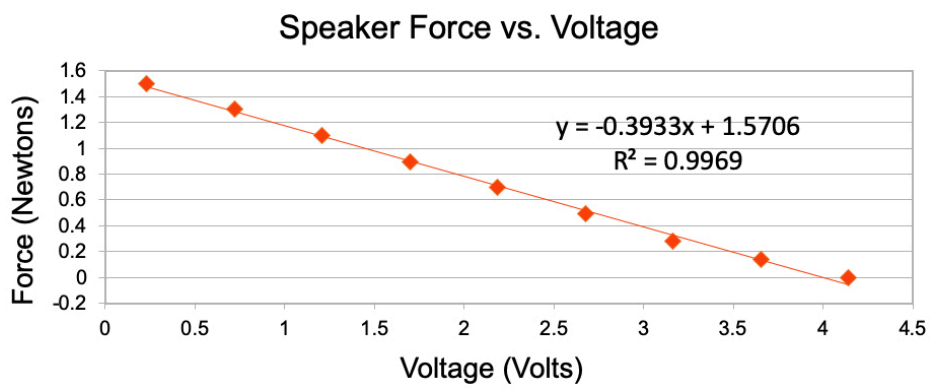


Figure 3

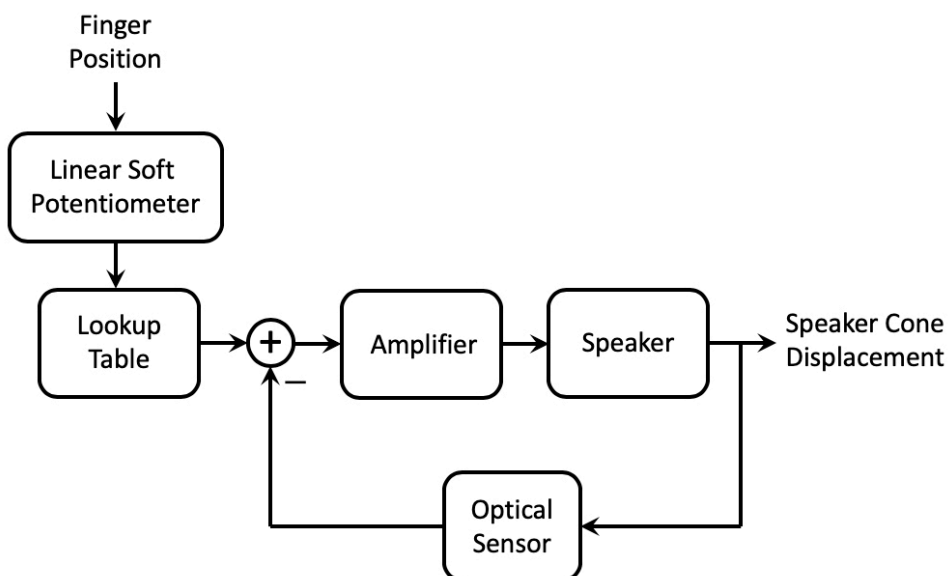


Figure 4

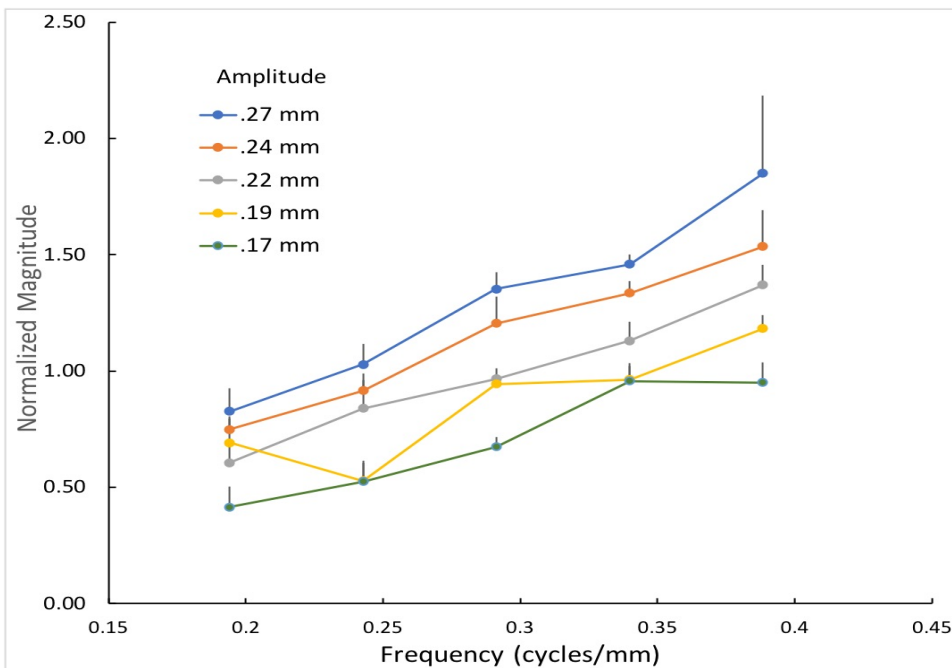


Figure 5

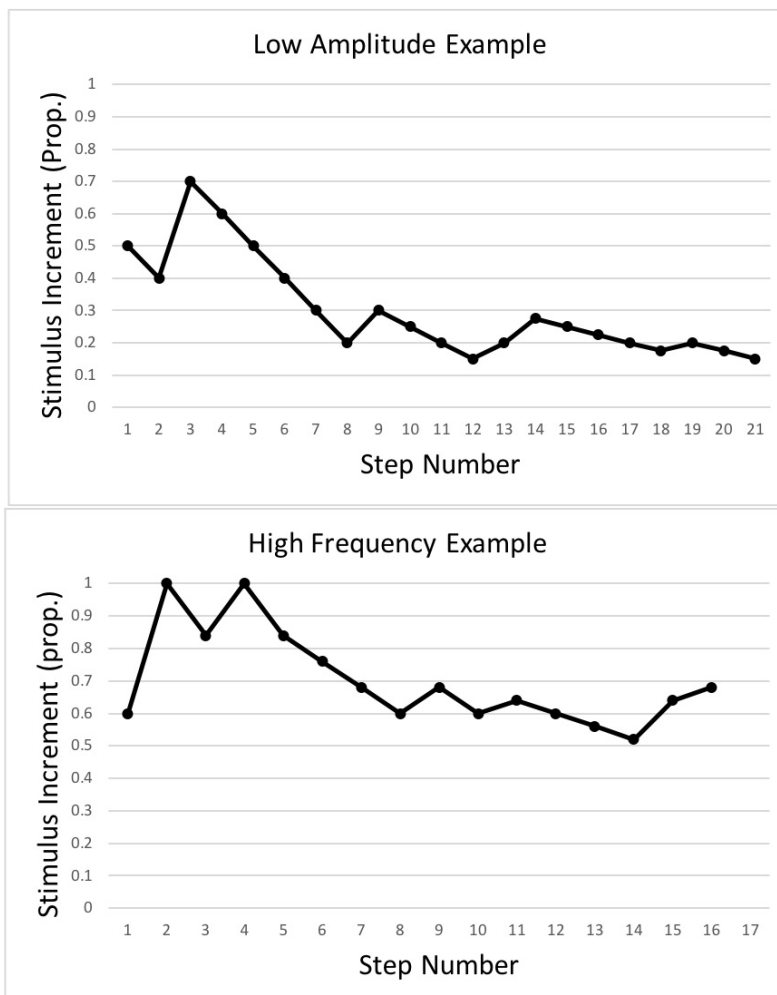


Figure 1. Device in operation showing rigid platform supporting the LSP mounted on the cone of a loudspeaker and positioning of the user's finger along the LSP.

Figure 2. Calibration data for loudspeaker force vs. voltage showing linear relationship over small displacement typical of texture rendering.

Figure 3. Control feedback loop demonstrating how the user's finger movement is transformed through a lookup table into a change in the speaker's cone height, as measured by the optical sensor.

Figure 4. Normalized magnitude estimation for each combination of frequency and peak-to-peak amplitude. Error bars are 1 s.e.m.

Figure 5. Sample traces from two participants in the low-amplitude and high-frequency conditions. Shown is the proportion increment relative to baseline at each step.